

## Inhibition of $\gamma$ -Secretase Activity by Helical $\beta$ -Peptide Foldamers

Yuki Imamura,<sup>†</sup> Naoto Watanabe,<sup>‡</sup> Naoki Umezawa,<sup>\*,†</sup> Takeshi Iwatsubo,<sup>‡,¶,§</sup>  
Nobuki Kato,<sup>†</sup> Taisuke Tomita,<sup>\*,‡,¶</sup> and Tsunehiko Higuchi<sup>\*,†</sup>

Graduate School of Pharmaceutical Sciences, Nagoya City University, 3-1 Tanabe-dori, Mizuho-ku, Nagoya, Aichi 467-8603, and Graduate School of Pharmaceutical Sciences, Core Research for Evolutional Science and Technology (CREST), Japan Science and Technology Corporation, and Graduate School of Medicine, The University of Tokyo, 7-3-1 Hongo, Bunkyo-ku, Tokyo 113-0033

Received January 8, 2009; E-mail: umezawa@phar.nagoya-cu.ac.jp; taisuke@mol.f.u-tokyo.ac.jp; higuchi@phar.nagoya-cu.ac.jp

**Abstract:** Alzheimer's disease (AD) is a neurodegenerative disorder pathologically characterized by extensive extracellular deposition of amyloid- $\beta$  (A $\beta$ ) peptides as senile plaques, and inhibition of "amyloidogenic" amyloid precursor protein (APP) processing by  $\gamma$ -secretase is an important strategy for prevention and treatment of AD. Here we show that  $\beta$ -peptide foldamers designed to adopt a 12-helical conformation in solution are potent and specific inhibitors of  $\gamma$ -secretase. Subtle modifications that disrupt helicity substantially reduce inhibitory potency, suggesting that helical conformation is critical for effective inhibition. These  $\beta$ -peptides competed with helical peptide-type inhibitor, suggesting that they interact with the substrate binding site of  $\gamma$ -secretase. The  $\beta$ -peptide with inhibitory activity at nanomolar concentration should be a useful lead compound for development of  $\gamma$ -secretase-specific inhibitors and molecular tools to explore substrate recognition by intramembrane proteases.

### Introduction

Alzheimer's disease (AD) is a neurodegenerative disorder that is characterized by extracellular deposition of amyloid- $\beta$  (A $\beta$ ) peptides as senile plaques.<sup>1,2</sup>  $\gamma$ -Secretase, a membrane-embedded aspartic protease comprising presenilin (PS), nicastrin, Aph-1 and Pen-2, is responsible for the proteolytic processing of amyloid precursor protein (APP) within the transmembrane domain to generate A $\beta$  peptides. Thus, inhibition or modulation of  $\gamma$ -secretase activity is a potentially effective strategy for the treatment of AD.<sup>3,4</sup> A number of  $\gamma$ -secretase inhibitors (GSIs) have been identified, including peptidic transition-state analogues (TSAs) that directly block the active site.<sup>3,4</sup>  $\alpha$ -Aminoisobutyric acid (Aib)-based helical peptides designed to mimic the APP transmembrane domain also inhibit  $\gamma$ -secretase activity by targeting the initial substrate docking site.<sup>5,6</sup> We hypothesized that unnatural oligomers with well-defined conformations ("foldamers")<sup>7–9</sup> can mimic the helical APP transmembrane domain and thereby inhibit  $\gamma$ -secretase activity. Here, we

describe the development of oligomers of  $\beta$ -amino acids (" $\beta$ -peptides") that interact with the substrate docking site of  $\gamma$ -secretase.  $\beta$ -Peptides are attractive unnatural scaffolds, because they adopt predictable helical conformations<sup>8,10</sup> and resist proteolysis.<sup>11,12</sup> Also, their oligomeric nature makes combinatorial design straightforward.

### Results and Discussion

**Foldamer Design and Secondary Structure Analysis.** We designed simple oligomers of conformationally restricted  $\beta$ -amino acids,  $\beta$ -peptides **1–6** (Figure 1). Enantiomers of trans-2-aminocyclopentanecarboxylic acid (ACPC) were chosen as the building blocks since their oligomers are fairly hydrophobic;  $\gamma$ -secretase cleaves hydrophobic membrane protein. Also, the oligomers of enantiomerically pure ACPC form stable 12-helix structure (defined by 12-membered ring C=O(*i*) → H–N(*i*+3) hydrogen bonds), which could be a good mimic of the  $\alpha$ -helix in terms of overall shape.<sup>8,10,13</sup> CD spectra of **1–6** in methanol are presented in Figure 2.  $\beta$ -Peptides **1–3** display a shallow minimum at ~222 nm and a maximum at 204–205 nm, which

<sup>†</sup> Nagoya City University.

<sup>‡</sup> Graduate School of Pharmaceutical Sciences, The University of Tokyo.

<sup>¶</sup> CREST.

<sup>§</sup> Graduate School of Medicine, The University of Tokyo.

- (1) Selkoe, D. J. *J. Clin. Invest.* **2002**, *110*, 1375–1381.
- (2) Wolfe, M. S. *Nat. Rev. Drug Discov.* **2002**, *1*, 859–866.
- (3) Tomita, T.; Iwatsubo, T. *Curr. Pharm. Des.* **2006**, *12*, 661–670.
- (4) Wolfe, M. S. *Neurotherapeutics* **2008**, *5*, 391–398.
- (5) Das, C.; Berezovska, O.; Diehl, T. S.; Genet, C.; Buldyrev, I.; Tsai, J. Y.; Hyman, B. T.; Wolfe, M. S. *J. Am. Chem. Soc.* **2003**, *125*, 11794–11795.
- (6) Kornilova, A. Y.; Bihel, F.; Das, C.; Wolfe, M. S. *Proc. Natl. Acad. Sci. U.S.A.* **2005**, *102*, 3230–3235.
- (7) Gellman, S. H. *Acc. Chem. Res.* **1998**, *31*, 173–180.

- (8) Cheng, R. P.; Gellman, S. H.; DeGrado, W. F. *Chem. Rev.* **2001**, *101*, 3219–3232.

- (9) Hill, D. J.; Mio, M. J.; Prince, R. B.; Hughes, T. S.; Moore, J. S. *Chem. Rev.* **2001**, *101*, 3893–4012.
- (10) Lee, H.-S.; Syud, F. A.; Wang, X.; Gellman, S. H. *J. Am. Chem. Soc.* **2001**, *123*, 7721–7722.
- (11) Frackepohl, J.; Arvidsson, P. I.; Schreiber, J. V.; Seebach, D. *ChemBioChem* **2001**, *2*, 445–55.
- (12) Porter, E. A.; Weisblum, B.; Gellman, S. H. *J. Am. Chem. Soc.* **2002**, *124*, 7324–7330.
- (13) Appella, D. H.; Christianson, L. A.; Klein, D. A.; Powell, D. R.; Huang, X.; Barchi, J. J., Jr.; Gellman, S. H. *Nature* **1997**, *387*, 381–384.

Peptides	Sequence	Number of $\beta$ -amino acids
1	Ac-X <sup>R</sup> X <sup>R</sup> X <sup>R</sup> X <sup>R</sup> X <sup>R</sup> X <sup>R</sup> -NH <sub>2</sub>	6
2	Ac-X <sup>R</sup> X <sup>R</sup> X <sup>R</sup> X <sup>R</sup> X <sup>R</sup> X <sup>R</sup> X <sup>R</sup> X <sup>R</sup> -NH <sub>2</sub>	9
3	Ac-X <sup>R</sup> X <sup>R</sup> X <sup>R</sup> X <sup>R</sup> X <sup>R</sup> X <sup>R</sup> X <sup>R</sup> X <sup>R</sup> X <sup>R</sup> X <sup>R</sup> -NH <sub>2</sub>	12
4	Ac-X <sup>S</sup> X <sup>S</sup> X <sup>S</sup> X <sup>S</sup> X <sup>S</sup> X <sup>S</sup> -NH <sub>2</sub>	6
5	Ac-X <sup>S</sup> X <sup>S</sup> X <sup>S</sup> X <sup>S</sup> X <sup>S</sup> X <sup>S</sup> X <sup>S</sup> X <sup>S</sup> -NH <sub>2</sub>	9
6	Ac-X <sup>S</sup> X <sup>S</sup> X <sup>S</sup> X <sup>S</sup> X <sup>S</sup> X <sup>S</sup> X <sup>S</sup> X <sup>S</sup> X <sup>S</sup> X <sup>S</sup> -NH <sub>2</sub>	12

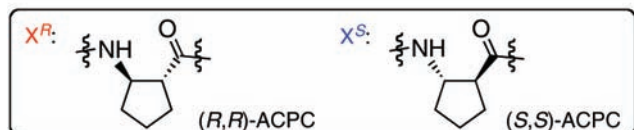


Figure 1. Synthesized helical  $\beta$ -peptide foldamers.

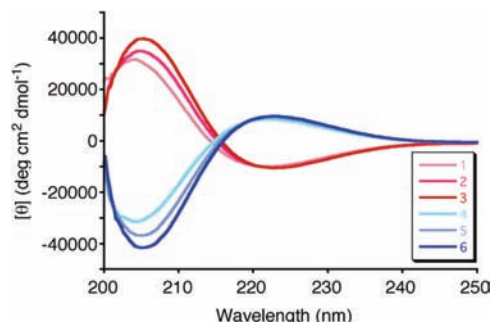


Figure 2. CD spectra of  $\beta$ -peptides 1–6 in methanol. The molar ellipticity  $[\theta]$  values have been normalized for oligomer concentration and the number of backbone amide groups.

Table 1. Inhibitory Potency of  $\beta$ -Peptides 1–6 toward  $\gamma$ -Secretase

compound	IC <sub>50</sub> (A $\beta$ 40, nM)	IC <sub>50</sub> (A $\beta$ 42, nM)
1	$>3.00 \times 10^4$	$>3.00 \times 10^4$
2	$2.87 \times 10^3$	$>3.00 \times 10^4$
3	$9.78 \times 10^2$	$1.23 \times 10^4$
4	$>3.00 \times 10^4$	$>3.00 \times 10^4$
5	19.8	$3.77 \times 10^3$
6	5.24	6.93

are characteristic of left-handed 12-helical  $\beta$ -peptides.<sup>13–15</sup> The increase in intensity at 222 nm with additional ACPC residues indicates that the population of the 12-helical state increases as the  $\beta$ -peptide length increases.  $\beta$ -Peptides 4–6 had mirror-image CD spectra compared with their enantiomers 1–3, within experimental error.

**$\gamma$ -Secretase Inhibitory Potency *in Vitro*.** The inhibitory potency of  $\beta$ -peptides was measured using an *in vitro* assay (Table 1).<sup>16</sup> ELISA quantification of *de novo* generated A $\beta$ 40 and A $\beta$ 42 from recombinant substrates was performed in the presence of  $\beta$ -peptides. For comparison, the inhibitory activity of benchmark GSIs and their photoactivatable derivatives,<sup>5,6,17–22</sup>

Table 2. Inhibitory Activity of Benchmark GSIs and Their Photoactivatable Derivatives Used in This Study in *in Vitro* Assay ( $n = 3$ )

class	compounds	IC <sub>50</sub> for A $\beta$ 40 (nM)	IC <sub>50</sub> for A $\beta$ 42 (nM)
helical peptide	pep.11 <sup>a</sup>	$6.67 \times 10^3$	$6.83 \times 10^3$
	pep.11-Bt	37.9	12.8
transition state analogue (TSA)	L-685,458	$4.68 \times 10^{-1}$	$5.48 \times 10^{-1}$
	31C	40.2	32.1
dipeptidic inhibitor	31C-Bpa	44.6	37.5
	DAPT	$1.73 \times 10^2$	$2.56 \times 10^2$
	compound E (CE)	$7.54 \times 10^{-1}$	$5.28 \times 10^{-1}$
	DBZ (YO01027)	$5.82 \times 10^{-1}$	$4.71 \times 10^{-1}$

<sup>a</sup> The difference in the potency of pep.11 compared with the previous report<sup>5</sup> may be due to the difference in the protocol of the *in vitro* assay system.

Peptides	Sequence	Number of $\beta$ -amino acids
7	Ac-X <sup>S</sup> X <sup>S</sup> X <sup>S</sup> X <sup>S</sup> X <sup>S</sup> X <sup>S</sup> X <sup>R</sup> X <sup>S</sup> X <sup>S</sup> X <sup>S</sup> X <sup>S</sup> -NH <sub>2</sub>	12
8	Ac-X <sup>S</sup> X <sup>S</sup> X <sup>S</sup> X <sup>R</sup> X <sup>S</sup> X <sup>S</sup> X <sup>S</sup> X <sup>S</sup> X <sup>R</sup> X <sup>S</sup> X <sup>S</sup> X <sup>S</sup> -NH <sub>2</sub>	12

Figure 3. Synthesized helicity-disrupted  $\beta$ -peptides.

which are discussed in the Mode of Action section, was also examined (Table 2; see Supporting Information for chemical structures). The inhibitory activity became stronger with increasing  $\beta$ -peptide length; hexamers (1 and 4) showed no activity, whereas dodecamers (3 and 6) showed the strongest activity in this series of enantiomers. Interestingly, the  $\beta$ -peptides composed of (*S,S*)-ACPC were much more potent inhibitors than those composed of (*R,R*)-ACPC. A similar tendency was observed in the case of helical peptide inhibitors: D-peptides were more potent than their L-peptide counterparts.<sup>5,23</sup> In the case of  $\beta$ -peptides, the right-handed helices 4–6 were more effective than the left-handed helices 1–3 ( $\beta$ -peptides composed of (*R,R*)-ACPC were reported to form left-handed 12-helix<sup>14</sup>). This is the opposite tendency to what was seen with helical  $\alpha$ -peptides: left-handed helical D-peptides were more potent than the right-handed L-peptides.<sup>5,23</sup> In the case of  $\alpha$ -peptides, the advantage of D-peptides may arise from their resistance to proteolytic degradation. For the  $\beta$ -peptides, there is not an issue of proteolysis, so the observed preference might reflect the intrinsic substrate preference of the  $\gamma$ -secretase. Among the compounds tested, 6 showed the strongest inhibitory activity, being comparable to the benchmark GSIs.

**Helicity-Disrupted  $\beta$ -Peptides.** To test whether these peptides inhibit  $\gamma$ -secretase simply owing to their hydrophobicity or whether conformation is critical, we designed and synthesized helicity-disrupted  $\beta$ -peptides 7 and 8 by swapping one or two (*S,S*)-ACPC residue(s) for (*R,R*)-ACPC residue(s) (Figure 3). CD spectra of  $\beta$ -peptides 6–8 in methanol are presented in Figure 4. The decrease in intensity at 222 nm with additional

- (14) Applequist, J.; Bode, K. A.; Appella, D. H.; Christianson, L. A.; Gellman, S. H. *J. Am. Chem. Soc.* **1998**, *120*, 4891–4892.  
 (15) Appella, D. H.; Christianson, L. A.; Klein, D. A.; Richards, M. R.; Powell, D. R.; Gellman, S. H. *J. Am. Chem. Soc.* **1999**, *121*, 7574–7581.  
 (16) Karlstrom, H.; Bergman, A.; Lendahl, U.; Naslund, J.; Lundkvist, J. *J. Biol. Chem.* **2002**, *277*, 6763–6766.  
 (17) Fuwa, H.; Takahashi, Y.; Konno, Y.; Watanabe, N.; Miyashita, H.; Sasaki, M.; Natsugari, H.; Kan, T.; Fukuyama, T.; Tomita, T.; Iwatsubo, T. *ACS Chem. Biol.* **2007**, *2*, 408–418.  
 (18) Morohashi, Y.; Kan, T.; Tominari, Y.; Fuwa, H.; Okamura, Y.; Watanabe, N.; Sato, C.; Natsugari, H.; Fukuyama, T.; Iwatsubo, T.; Tomita, T. *J. Biol. Chem.* **2006**, *281*, 14670–14676.

- (19) Kan, T.; Tominari, Y.; Morohashi, Y.; Natsugari, H.; Tomita, T.; Iwatsubo, T.; Fukuyama, T. *Chem. Commun.* **2003**, 2244–2245.  
 (20) Esler, W. P.; Kimberly, W. T.; Ostaszewski, B. L.; Ye, W.; Diehl, T. S.; Selkoe, D. J.; Wolfe, M. S. *Proc. Natl. Acad. Sci. U.S.A.* **2002**, *99*, 2720–2725.  
 (21) Dovey, H. F.; et al. *J. Neurochem.* **2001**, *76*, 173–181.  
 (22) Li, Y. M.; Xu, M.; Lai, M. T.; Huang, Q.; Castro, J. L.; DiMuzio-Mower, J.; Harrison, T.; Lellis, C.; Nadin, A.; Neduveilil, J. G.; Register, R. B.; Sardana, M. K.; Shearman, M. S.; Smith, A. L.; Shi, X. P.; Yin, K. C.; Shafer, J. A.; Gardell, S. J. *Nature* **2000**, *405*, 689–694.  
 (23) Bihel, F.; Das, C.; Bowman, M. J.; Wolfe, M. S. *J. Med. Chem.* **2004**, *47*, 3931–3933.

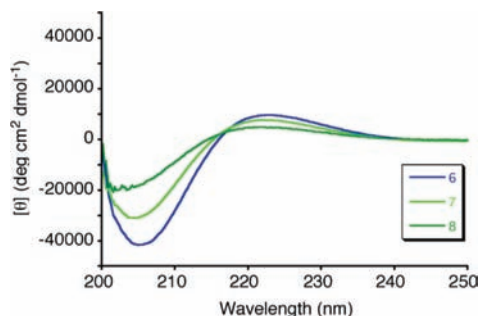


**Figure 4.** CD spectra of  $\beta$ -peptides 6–8 in methanol. The molar ellipticity  $[\theta]$  values have been normalized for oligomer concentration and the number of backbone amide groups.

**Table 3.** Inhibitory Potency of  $\beta$ -Peptides 7–8 toward  $\gamma$ -Secretase

compound	IC <sub>50</sub> (A $\beta$ 40, nM)	IC <sub>50</sub> (A $\beta$ 42, nM)
7	$6.89 \times 10^3$	$>3.00 \times 10^4$
8	$>3.00 \times 10^4$	$>3.00 \times 10^4$

**Table 4.** Inhibitory Potency of GSIs on HEK293/SC100gal4 Cells ( $n = 3$ )

class	compounds	IC <sub>50</sub> for A $\beta$ 40 (nM)	IC <sub>50</sub> for A $\beta$ 42 (nM)	IC <sub>50</sub> for AICD (nM)
helical peptide	pep.11	$>1.00 \times 10^4$	$>1.00 \times 10^4$	$7.84 \times 10^3$
TSA	L-685,458	$5.48 \times 10^3$	$1.51 \times 10^4$	$1.61 \times 10^3$
dipeptidic inhibitor	DAPT	$2.45 \times 10^3$	57.4% <sup>a</sup>	$4.70 \times 10^2$
$\beta$ -peptide	6	70.6	82.0	4.88

<sup>a</sup> Inhibition of 57.4% was observed at 30000 nM.

**Table 5.** Inhibitory Potency of GSIs on N2a cells ( $n = 3$ )

class	compounds	IC <sub>50</sub> for A $\beta$ 40 (nM)	IC <sub>50</sub> for A $\beta$ 42 (nM)
helical peptide	pep.11	$>1.00 \times 10^4$	$>1.00 \times 10^4$
TSA	L-685,458	$7.57 \times 10^2$	$4.10 \times 10^3$
dipeptidic inhibitor	DAPT	$8.63 \times 10^2$	$1.93 \times 10^3$
$\beta$ -peptide	6	95.6	$2.21 \times 10^2$

(*R,R*)-ACPC replacements indicates that the population of the 12-helical state decreases as the number of (*R,R*)-ACPC residues increases. Replacement of a single monomer unit led to significant loss of inhibitory potency compared with the corresponding enantiomer (Table 3), suggesting that helical character is critical for the inhibitory potency of 12-helical  $\beta$ -peptides.

**Cell-Based Assay.** Next the inhibitory potency of  $\beta$ -peptides was measured using cell-based assay. ELISA quantifications of secreted A $\beta$ 40 and A $\beta$ 42 from HEK293/SC100gal4<sup>24</sup> (Table 4) or Neuro2a<sup>25</sup> cells (Table 5) in the presence of  $\beta$ -peptides were performed. The release of APP intracellular domain (AICD), a counterpart of A $\beta$ , was also analyzed by Gal4-fused AICD-driven UAS-firefly luciferase activity in HEK293/SC100gal4 cells.<sup>24</sup> We found that 6 showed most potent inhibitory activity both in A $\beta$  and AICD generation. Increase in the A $\beta$  secretion (“A $\beta$  rise”) at low concentration of 6 was observed in a similar manner to that by benchmark GSIs,<sup>26</sup>

presumably due to the aberrant trafficking and processing of the accumulated  $\gamma$ -secretase substrates (Figure 5). Finally, we confirmed that 6 inhibited the A $\beta$  secretion accompanied with the accumulation of C-terminal stubs of endogenous APP in primary neuronal culture (Figure 6). These results suggest that the  $\beta$ -peptide directly targets the  $\gamma$ -secretase *in vivo*.

**Specificity of  $\beta$ -Peptide.** There is serious concern about adverse effects caused by GSIs that inhibit the release of Notch intracellular domain (NICD), a direct signaling molecule in the Notch pathway.<sup>1–4</sup> Thus, identification of a way to spare Notch-cleaving  $\gamma$ -secretase activity is considered mandatory for development of AD therapeutics. We examined the effect of  $\beta$ -peptides 5 and 6 on Notch cleavage in PS1-expressing #5/DKO cells (Table 6), which coexpress truncated APP and Notch with the corresponding luciferase reporter system (i.e., Gal4/VP16-fused AICD-driven UAS-firefly luciferase and NICD-driven TP1-*Renilla* luciferase, respectively). Intriguingly, both 5 and 6, but not benchmark GSI DBZ, preferentially inhibited AICD over NICD generation, suggesting that the  $\beta$ -peptides show substrate specificity in a fashion similar to that of Notch-sparing GSI.<sup>27</sup> Then, we examined whether the  $\beta$ -peptides affect other proteases which target hydrophobic substrates, since the  $\beta$ -peptides are relatively hydrophobic. Treatment with 6 caused no significant change in the levels of sAPP $\alpha$  generated by  $\alpha$ -secretase activity, suggesting that the  $\beta$ -peptide 6 had no effect on the membrane-bound metalloproteases ADAM9, -10, and -17 (Figure. 7).<sup>28</sup> Next, we tested the effect of  $\beta$ -peptide on the intramembrane cleaving protease, signal peptide peptidase (SPP). TSA-based GSI cross-inhibited the SPP activity, because PS and SPP share catalytic YD/GxGD motifs.<sup>29</sup> Moreover, we and others have reported that potent dipeptidic GSIs such as DBZ, but not DAPT, cross-inhibit SPP.<sup>17,30,31</sup> It is noteworthy that leucine-rich Aib containing helical peptides cross-inhibited the  $\gamma$ -secretase and SPP activities, but these compounds showed some preference for SPP activity.<sup>32,33</sup> These data suggest that the  $\gamma$ -secretase and SPP execute intramembrane cleavage with similar, but not identical, mechanisms. Unexpectedly, 6 had no effect on the SPP activity in cell-based assay, while 6 exhibited inhibitory activity against AICD generation comparable to that of DBZ (Table 6, Figure 8). Taken together, these data suggest that  $\beta$ -peptide 6 is one of the most potent peptide-based GSIs found thus far and represents a potential lead compound for the development of APP-cleaving  $\gamma$ -secretase activity-specific inhibitors.

**Mode of Action.** PS undergoes endoproteolysis to generate N-terminal and C-terminal fragments (NTF and CTF, respectively) in active  $\gamma$ -secretase complex.<sup>1–4,34</sup> Using pharmacologically distinct photoactivatable GSI derivatives, it is now widely accepted that (1) PS fragments represent the proteolytically active molecule, (2) PS fragments form an initial substrate docking site distinct from the catalytic site of the  $\gamma$ -secretase,

(27) Mayer, S. C.; et al. *J. Med. Chem.* **2008**, *51*, 7348–7351.

(28) Deuss, M.; Reiss, K.; Hartmann, D. *Curr. Alzheimer Res.* **2008**, *5*, 187–201.

(29) Fluhrer, R.; Haass, C. *Neurodegener. Dis.* **2007**, *4*, 112–116.

(30) Nyborg, A. C.; Jansen, K.; Ladd, T. B.; Fauq, A.; Golde, T. E. *J. Biol. Chem.* **2004**, *279*, 43148–43156.

(31) Weihofen, A.; Lemberg, M. K.; Friedmann, E.; Rueeger, H.; Schmitz, A.; Paganetti, P.; Rovelli, G.; Martoglio, B. *J. Biol. Chem.* **2003**, *278*, 16528–16533.

(32) Sato, T.; Ananda, K.; Cheng, C. I.; Suh, E. J.; Narayanan, S.; Wolfe, M. S. *J. Biol. Chem.* **2008**, *283*, 33287–33295.

(33) Sato, T.; Nyborg, A. C.; Iwata, N.; Diehl, T. S.; Saido, T. C.; Golde, T. E.; Wolfe, M. S. *Biochemistry* **2006**, *45*, 8649–8656.

(34) Selkoe, D. J.; Wolfe, M. S. *Cell* **2007**, *131*, 215–221.

(24) Isoo, N.; Sato, C.; Miyashita, H.; Shinohara, M.; Takasugi, N.; Morohashi, Y.; Tsuji, S.; Tomita, T.; Iwatsubo, T. *J. Biol. Chem.* **2007**, *282*, 12388–12396.

(25) Tomita, T.; Maruyama, K.; Saido, T. C.; Kume, H.; Shinozaki, K.; Tokuhira, S.; Capell, A.; Walter, J.; Grunberg, J.; Haass, C.; Iwatsubo, T.; Obata, K. *Proc. Natl. Acad. Sci. U.S.A.* **1997**, *94*, 2025–2030.

(26) Burton, C. R.; et al. *J. Biol. Chem.* **2008**, *283*, 22992–23003.

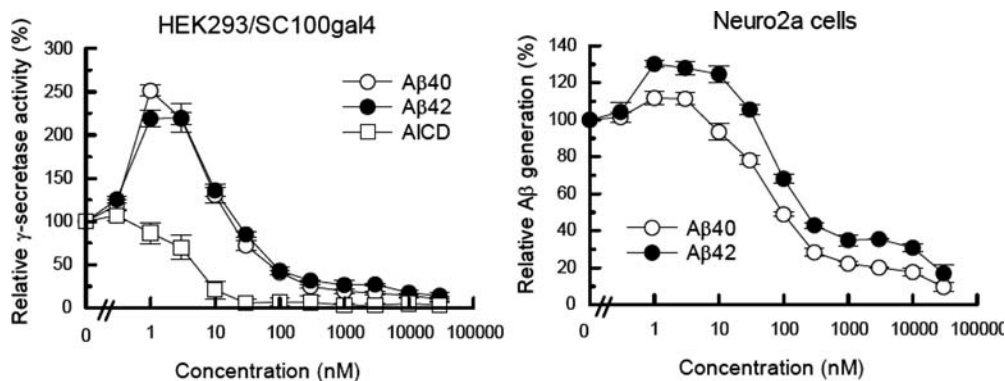


Figure 5. Inhibitory effect of **6** on cell-based  $\gamma$ -secretase activity.

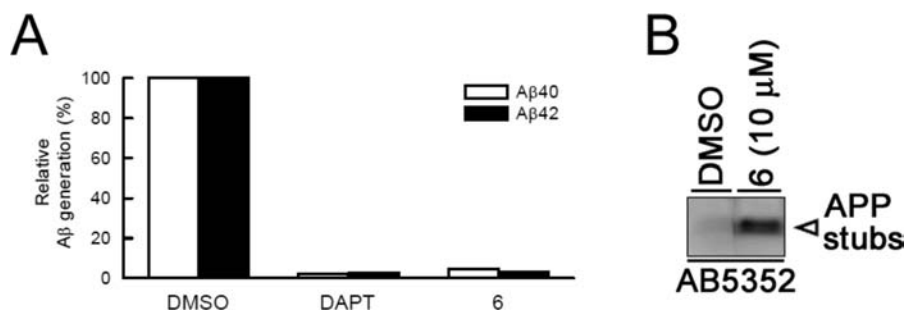


Figure 6. Inhibitory effect of **6** on the  $\gamma$ -secretase activity in primary neuronal culture. (A) The levels of the secreted  $A\beta$  measured by ELISA. Concentration of DAPT or  $\beta$ -peptide **6** was  $10 \mu\text{M}$  ( $n = 4$ , S.E.). (B) Detection of endogenous APP C-terminal stubs (white arrowhead) by immunoblotting with anti-APP antibody AB5352.

Table 6. Inhibitory Potency of GSIs on PS1 Expressing #5/DKO cells ( $n = 3$ )

class	compounds	IC <sub>50</sub> for AICD (nM)	IC <sub>50</sub> for NICD (nM)	notch selectivity
dipeptidic inhibitor	DBZ	2.90	1.54	0.5
$\beta$ -peptide	<b>5</b>	44.7	$5.64 \times 10^2$	12.6
	<b>6</b>	3.70	18.9	5.1

(3) Substrates are transferred from the docking to the catalytic site through a transition path (see Figure 10A).<sup>18</sup> To elucidate the mode of action of the  $\beta$ -peptides, we examined the ability of these peptides to displace photoactivatable GSIs in a photoaffinity experiment. The labeling of PS1 NTF by Aib-containing helical pep.11-Bt, which directly targets the initial substrate docking site,<sup>6</sup> was completely abolished by preincubation with **5** or **6** (Figure 9A), suggesting that these  $\beta$ -peptides share the same binding site with pep.11. Unexpectedly, the biotinylation of PS1 by TSA-based photoprobe 31C-Bpa, that directly bound to the catalytic site,<sup>35</sup> was somewhat decreased by the  $\beta$ -peptides, while pep.11 increased the labeling of PS1

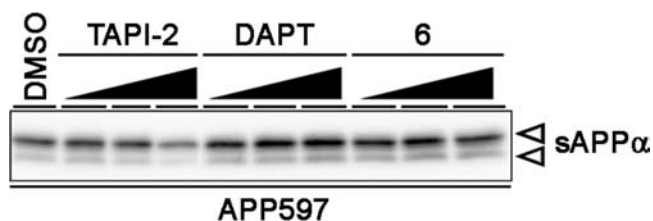


Figure 7. Effect of **6** on the levels of the sAPP $\alpha$  secreted from Neuro2a cells. sAPP $\alpha$  (white arrowheads) was detected by immunoblotting using anti-APP ectodomain APP597. Black triangles on the lanes schematically represent concentrations of the inhibitors. TAPI-2 is a representative metalloprotease inhibitor.

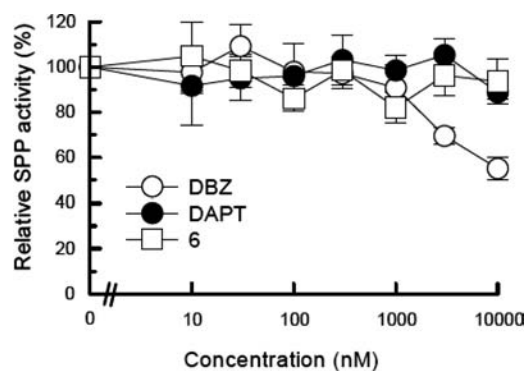


Figure 8. Inhibitory effect of **6** on the SPP activity in cell-based assay.

(Figure 9B).<sup>6</sup> Next the effects of the  $\beta$ -peptides on the biotinylation by dipeptidic photoprobes (i.e., DAP-BpB and CE-BpB3) were examined.<sup>17,18</sup> Pep.11 decreased the biotinylation of PS1 by DAP-BpB, while the labeling by CE-BpB3 was increased as previously described.<sup>17,36</sup> In contrast, the  $\beta$ -peptides increased the labeling of PS1 by both DAP-BpB and CE-BpB3, suggesting that the  $\beta$ -peptides conferred an open conformation to the transit path. Taken together, these data support our notion that the  $\beta$ -peptides target the initial substrate docking site of the  $\gamma$ -secretase in a different fashion compared with pep.11.

A schematic depiction of  $\gamma$ -secretase cleavage is shown in Figure 10A.<sup>17,18</sup> Catalytic aspartates are shown as red circles

(35) Micchelli, C. A.; Esler, W. P.; Kimberly, W. T.; Jack, C.; Berezovska, O.; Kornilova, A.; Hyman, B. T.; Perrimon, N.; Wolfe, M. S. *FASEB J.* **2003**, *17*, 79–81.

(36) Takahashi, Y.; Hayashi, I.; Tominari, Y.; Rikimaru, K.; Morohashi, Y.; Kan, T.; Natsugari, H.; Fukuyama, T.; Tomita, T.; Iwatsubo, T. *J. Biol. Chem.* **2003**, *278*, 18664–18670.

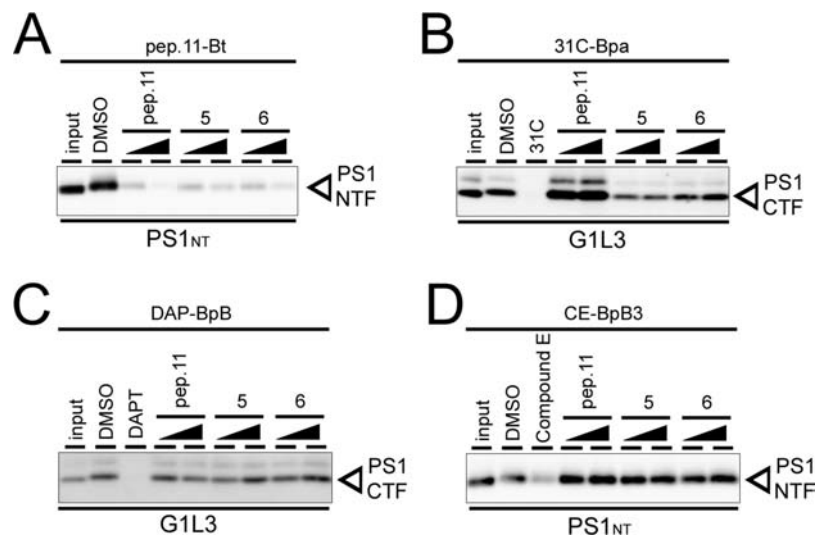


**Figure 9.** Competition assay against photoaffinity labeling with pep.11-Bt (A), 31C-Bpa (B), DAP-BpB (C), and CE-BpB3 (D) in the presence of pep.11 or  $\beta$ -peptide 5 or 6. The biotinylated PS1 fragments (white arrowheads) were detected by immunoblotting using antibodies against PS1 N terminus and loop region (PS1NT and G1L3, respectively). Black triangles on the lanes schematically represent concentrations of the competitors.

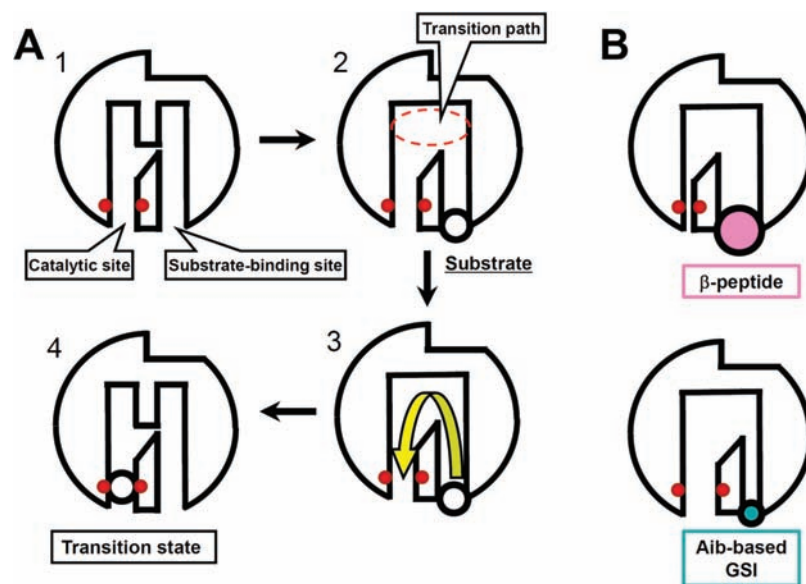


**Figure 10.** Proposed mechanism of the  $\gamma$ -secretase cleavage and the effects of helical peptides. (A) Schematic depiction of the  $\gamma$ -secretase cleavage. (B) Putative inhibition modes of the  $\beta$ -peptide and Aib-based GSI.

at the catalytic site. Substrates enter the  $\gamma$ -secretase from the initial substrate docking site to the catalytic site through the transition path. In Figure 10B, putative inhibition modes of the  $\beta$ -peptide and Aib-based GSI are proposed. Both helical peptides target the initial substrate docking site. However, the occupation of the substrate binding site by the  $\beta$ -peptides allosterically narrows the catalytic site, while the binding of Aib-based GSI enlarges the conformational space of the catalytic site. These steric changes affected the labeling efficacy of PS1 by a photoprobe based on the transition-state analogue, 31C-Bpa, which directly targets the catalytic site.

## Conclusion

We have shown that a simple  $\beta$ -peptide foldamer acts as a highly potent GSI and that helical conformation is critical for this inhibition.  $\beta$ -Peptides composed of ACPC exhibit a strong tendency to adopt a specific helical conformation, 12-helix, and therefore may display side chains in predictable arrangements.

Intriguingly,  $\beta$ -peptide presented here specifically inhibited the  $\gamma$ -secretase activity with substrate preference. Moreover, a chemical biological approach revealed that  $\beta$ -peptides directly target the initial substrate docking site of the  $\gamma$ -secretase. The present helical  $\beta$ -peptide inhibitor with activity at nanomolar concentration is expected to be a good lead compound for the development of  $\gamma$ -secretase-specific inhibitors and molecular tools to explore the substrate recognition of intramembrane proteases.

## Experimental Section

**Synthesis of  $\beta$ -Peptides.** Fmoc-*trans*-2-aminocyclopentanecarboxylic acid (Fmoc-ACPC-OH) was synthesized according to the reported procedure.<sup>37</sup>  $\beta$ -Peptides were synthesized with standard Fmoc solid phase methods. Fmoc-NH-SAL-PEG resin (0.24 mmol/g, 100–200 mesh, 1% DVB) was employed for all peptide synthesis. For a typical 20  $\mu$ mol-scale synthesis: 83 mg of Fmoc-NH-SAL-PEG resin was swollen for 15 min in DMF. **Coupling**

**cycles.** Three equivalents of Fmoc-ACPC-OH and 3 equiv of 2-(1H-benzotriazol-1-yl)-1,1,3,3-tetramethyluronium hexafluorophosphate (HBTU) and 3 equiv of 1-hydroxybenzotriazole monohydrate (HOBt·H<sub>2</sub>O) were dissolved in 300  $\mu$ L of DMF, and 6 equiv of *N,N*-diisopropylethylamine (DIEA) was added. The solution was added to the resin bearing the N-deprotected  $\beta$ -peptide. The resin was agitated for 1–3 h. **Fmoc deprotection cycles.** Fmoc deprotection was accomplished by adding to the resin 1.0 mL of 20% (v/v) piperidine in DMF and rocking for 30 min. **Acetylation.** Acetylation of peptides was conducted for 2 h, by addition of 0.5 mL of 2:2:1 (v/v/v) Ac<sub>2</sub>O/DMF/Et<sub>3</sub>N to the resin bearing the final desired N-deprotected  $\beta$ -peptide sequence. **Cleavage.** Cleavage of all  $\beta$ -peptides from resin was accomplished by shaking the resin in a solution of trifluoroacetic acid (TFA)/triisopropylsilane (TIPS)/H<sub>2</sub>O 95:2.5:2.5 (0.5 mL) for 2 h. The resin was removed *via* filtration and rinsed with additional TFA. The combined filtrate was concentrated under a stream of Ar.  $\beta$ -Peptides were precipitated from excess cold Et<sub>2</sub>O, and isolated by centrifugation. The crude  $\beta$ -peptides thus obtained were purified by RP-HPLC using a linear gradient system from 30:70 to 70:30 isopropanol/H<sub>2</sub>O (0.1% TFA) over 40 min ( $\beta$ -peptides 1 and 4), from 45:55 to 65:35 isopropanol/H<sub>2</sub>O (0.1% TFA) over 45 min ( $\beta$ -peptides 2 and 5), from 50:50 to 65:35 isopropanol/H<sub>2</sub>O (0.1% TFA) over 45 min ( $\beta$ -peptides 3 and 6), from 40:60 to 55:45 isopropanol/H<sub>2</sub>O (0.1% TFA) over 45 min ( $\beta$ -peptide 7) at the flow rate of 2.1 mL/min. In the case of  $\beta$ -peptide 8, the crude  $\beta$ -peptide was dissolved in formic acid and purified by RP-HPLC using a linear gradient of 70:30 to 95:5 methanol/H<sub>2</sub>O (0.1% TFA) over 45 min at the flow rate of 3.0 mL/min. The purities of  $\beta$ -peptides were ~95%, as measured by comparing peak areas in analytical HPLC traces at 220 nm (see Supporting Information).

**CD Spectra.** Dry peptide samples were weighed on a microanalytical balance and dissolved in an appropriate amount of HPLC-grade methanol. Sample cells of 10-mm path length were used. Data were collected on a Jasco J-725 spectropolarimeter at room temperature. Data were converted to mean residue ellipticity (deg cm<sup>2</sup> dmol<sup>-1</sup>) according to the following equation:

$$[\Theta] = \psi M_r / 100lc$$

where  $\psi$  is the CD signal in degrees,  $M_r$  is the molecular weight divided by the number of chromophores,  $l$  is the path length in decimeters, and  $c$  is the concentration in g/mL.

**Protocol of in Vitro and in Vivo Assay for Inhibitory Activity.** Inhibitory potencies of the  $\beta$ -peptides on the  $\gamma$ -secretase activity were analyzed by *in vitro* or cell-based assays. *In vitro*  $\gamma$ -secretase assay was performed as described previously with some modifications.<sup>36</sup> *N*-[*N*-(3,5-Difluorophenacetyl)-L-alanyl]-(*S*)-phenylglycine *tert*-butyl ester (DAPT) was a gift from Dr. Fukuyama (The University of Tokyo).<sup>19</sup> L-685,458, pep.11, pep.11-Bt and TAPI-2 were purchased from Bachem, Ito Lifescience, BEX and BIOMOL, respectively. Purified recombinant substrate (C100-FLAG-myc-6xHis) was incubated together with solubilized HeLa cell membrane fraction (250  $\mu$ g/mL) in  $\gamma$  buffer (HEPES buffer containing 0.25% CHAPSO, 5 mM EDTA, 5 mM 1,10-phenanthroline, 10 mg/mL phosphoramidon, 0.01% phosphatidylcholine (Avanti) and Complete protease inhibitor mixture (Roche Applied Science)) at 37 °C. The samples were centrifuged, and the supernatants were analyzed by BNT77/BA27 or BNT77/BC05 ELISAs for *de novo* generation of A $\beta$ . For cell-based assays, HEK293 cells stably overexpressing SC100gal4, EGFP and UAS-firefly luciferase (HEK293/SC100gal4) or Neuro2a cells were cultured in the presence of various concentrations of the compounds for 24 h. Primary neuronal culture from mouse embryo was obtained as previously described.<sup>38</sup> Neurons were cultured with GSIs at DIV 6 and incubated for 24 h. Cultured media were collected and

subjected to BNT77/BA27 or BNT77/BC05 ELISAs to measure the levels of secreted A $\beta$ . The levels of APP C-terminal stubs were analyzed by immunoblotting using anti-APP antibody AB5352 (Millipore). To analyze the effect on the sAPP $\alpha$  generation, Neuro2a cells were treated with TAPI-2 (0.2, 2, 20  $\mu$ M), DAPT (0.1, 1, 10  $\mu$ M) or **6** (0.1, 1, 10  $\mu$ M) for 24 h, and conditioned medium was subjected to immunoblotting against sAPP $\alpha$  (APP597, IBL, Japan). For generation of #5/DKO cells, retroviral expression vectors containing SPC99gvp-6myc (modified SPA4CT<sup>39</sup> fused with Gal4/VP16 and hexa-myc epitope tag) in pMXs-puro,<sup>40,41</sup> N $\Delta$ E-6myc (truncated mouse Notch<sup>42</sup> fused with hexa-myc epitope tag) in pLPCX (Clontech), UAS-firefly luciferase in pMXs-EGFP<sup>II</sup> and TP1-*Renilla* luciferase in pMXs-II were constructed. pMXs-EGFP<sup>II</sup> is a derivative encoding EGFP instead of puromycin resistance gene in pMXs-puroII.<sup>43</sup> pMXs-II was generated by an excision of puromycin resistance gene in pMXs-puroII. All plasmids were transfected into retrovirus packaging cell line, Plat-E.<sup>41</sup> Recombinant retroviruses were inoculated with immortalized fibroblasts obtained from *Psen1*<sup>-/-</sup>; *Psen2*<sup>-/-</sup> knockout mouse (DKO cells).<sup>44</sup> Infected DKO cells were further selected with puromycin to obtain #5/DKO cells as previously described.<sup>40,41</sup> Before GSI treatment, recombinant retrovirus encoding PS1 was infected into #5/DKO cells. The GSI-treated cell lysates were subjected to the luciferase assay to measure the AICD- and NICD-generating activity.<sup>24</sup>

**SPP Assay.** SPP reporter assay was performed as previously described.<sup>30</sup> HEK293 cells were transiently transfected with expression plasmids encoding *Renilla* luciferase, human SPP<sup>45</sup> and recombinant SPP substrate fused with ATF6<sup>30</sup> together with ERSE-firefly luciferase reporter vector.<sup>46</sup> The cell lysate was harvested after 24 h and subjected to the luciferase assay to measure SPP activity. The firefly luciferase activity was normalized to the *Renilla* luciferase activity control.

**Photoaffinity Labeling Study.** Photoaffinity labeling experiments were performed as previously described.<sup>17,18</sup> Compound E (CE) was purchased from Calbiochem or kindly provided by Dr. Haruhiko Fuwa (Tohoku University). 1% CHAPSO-solubilized HeLa cell membrane fractions were diluted to 0.25% CHAPSO and incubated with the photoaffinity probes (pep11-Bt; 100 nM, 31C-Bpa; 100 nM, DAP-BpB; 100 nM, CE-BpB3; 30 nM) at 4 °C. In the competition experiments, the solubilized membranes were mixed with the parent compounds (pep.11; 2.5 and 25  $\mu$ M, 31C; 10  $\mu$ M, DAPT; 10  $\mu$ M, Compound E; 3  $\mu$ M) or the  $\beta$ -peptides (**5**; 300 and 3000 nM, **6**; 30 and 300 nM), prior to the addition of the photoaffinity probe. The samples were irradiated on ice using a UV lamp. SDS was added to the labeled samples to give a final concentration of 1% w/v, and the solution was incubated with Dynabeads M-280 (Invitrogen). Biotinylated proteins were eluted from the resin by boiling for 1 min in Laemmli sample buffer. The labeled proteins were detected by immunoblotting using anti-

(37) LePlae, P. R.; Umezawa, N.; Lee, H.-S.; Gellman, S. H. *J. Org. Chem.* **2001**, *66*, 5629–5632.

(38) Fukumoto, H.; Tomita, T.; Matsunaga, H.; Ishibashi, Y.; Saido, T. C.; Iwatsubo, T. *Neuroreport* **1999**, *10*, 2965–2969.

(39) Lichtenthaler, S. F.; Multhaup, G.; Masters, C. L.; Beyreuther, K. *FEBS Lett.* **1999**, *453*, 288–292.

(40) Watanabe, N.; Tomita, T.; Sato, C.; Kitamura, T.; Morohashi, Y.; Iwatsubo, T. *J. Biol. Chem.* **2005**, *280*, 41967–41975.

(41) Kitamura, T.; Koshino, Y.; Shibata, F.; Oki, T.; Nakajima, H.; Nosaka, T.; Kumagai, H. *Exp. Hematol.* **2003**, *31*, 1007–1014.

(42) Kopan, R.; Schroeter, E. H.; Weintraub, H.; Nye, J. S. *Proc. Natl. Acad. Sci. U.S.A.* **1996**, *93*, 1683–1688.

(43) Kamura, T.; Hara, T.; Matsumoto, M.; Ishida, N.; Okumura, F.; Hatakeyama, S.; Yoshida, M.; Nakayama, K.; Nakayama, K. I. *Nat. Cell Biol.* **2004**, *6*, 1229–1235.

(44) Herreman, A.; Serneels, L.; Annaert, W.; Collen, D.; Schoonjans, L.; De Strooper, B. *Nat. Cell Biol.* **2000**, *2*, 461–462.

(45) Grigorenko, A. P.; Moliaka, Y. K.; Soto, M. C.; Mello, C. C.; Rogae, E. I. *Proc. Natl. Acad. Sci. U.S.A.* **2004**, *101*, 14955–14960.

(46) Yoshida, H.; Haze, K.; Yanagi, H.; Yura, T.; Mori, K. *J. Biol. Chem.* **1998**, *273*, 33741–33749.

PS1<sub>NT</sub><sup>47</sup> (kindly provided by Dr. Gopal Thinakaran, The University of Chicago) or anti-GIL3 antibody.<sup>48</sup>

**Acknowledgment.** We thank Drs. G. Thinakaran (The University of Chicago), B. De Strooper (KU Leuven), U. Strobl (Helmholtz Zentrum München), A. Nyborg, T. Golde (Mayo Clinic), A. P. Grigorenko, E. I. Rogaev (University of Massachusetts), H. Fuwa, M. Sasaki (Tohoku University), T. Kitamura, S. Yokoshima, T. Fukuyama (The University of Tokyo), K. Mori (Kyoto University), K. I. Nakayama (Kyushu University), R. Kopan (Washington University in St. Louis), Takeda Pharmaceutical Company and lab

- (47) Thinakaran, G.; Harris, C. L.; Ratovitski, T.; Davenport, F.; Slunt, H. H.; Price, D. L.; Borchelt, D. R.; Sisodia, S. S. *J. Biol. Chem.* **1997**, *272*, 28415–28422.
- (48) Tomita, T.; Takikawa, R.; Koyama, A.; Morohashi, Y.; Takasugi, N.; Saïdo, T. C.; Maruyama, K.; Iwatsubo, T. *J. Neurosci.* **1999**, *19*, 10627–10634.

members for valuable reagents, helpful discussions and technical assistance. We also thank Prof. H. Sajiki and Dr. Y. Monguchi (Gifu Pharmaceutical University) for HRMS-FAB analysis. This work was supported in part by Grants-in-Aid for Scientific Research (A) (T.H.), Young Scientists (S) from Japan Society for the Promotion of Science (JSPS) (T.T), by the Targeted Proteins Research Program of the Japan Science and Technology Corporation (JST) (T.I., T.T.), and Uehara Memorial Foundation (N.U.). N.W. was a research fellow of JSPS.

**Supporting Information Available:** Chemical structures of benchmark GSIs and their photoactivatable derivatives, identification of  $\beta$ -peptides **1–8**, synthesis of 31C-Bpa; complete refs 21, 26, and 27. This material is available free of charge via the Internet at <http://pubs.acs.org>.

JA9001458